Detection of a Formate Surface Intermediate in the Atomic Layer Deposition of High-κ Dielectrics Using Ozone

Jinhee Kwon,*,† Min Dai,‡ Mathew D. Halls,§ and Yves J. Chabal†

Laboratory for Surface Modification, Rutgers University, Piscataway, New Jersey 08854, Materials Science Division, Accelrys Inc., San Diego, California 92121, and Department of Materials Science and Engineering, University of Texas at Dallas, Richardson, Texas 75080

Received December 22, 2007
Revised Manuscript Received April 2, 2008

Trimethylaluminum (TMA, $Al(CH_3)_3$) is one of the most commonly used metal-organic sources in various industries. It is an important precursor for the preparation of III−V compound semiconductors[1] and has been used in catalytic applications for a long time.[2] More recently, TMA has been the main metal precursor for atomic layer deposition (ALD) of high dielectric gate oxide Al_2O_3 in real device integration.[3] Because of its importance in the microelectronics industry, numerous theoretical and experimental studies have been performed to characterize Al_2O_3 films grown by ALD with TMA and various oxygen sources.[4] In particular, the Al_2O_3 ALD process using TMA and water has been extensively studied and the reaction mechanisms are now well understood.

Due to its inherent high reactivity and volatility, O_3 is currently under investigation as an alternative oxygen precursor for ALD applications. One of the motivations for using O_3 is the desire to greatly reduce the incorporation of impurities, such as hydroxyl ions (OH^-) in the resulting film.[5] Some studies have reported superior structural and electronic properties for metal-oxide films deposited using O_3 sources in comparison to those deposited using H_2O.[6] However, under similar reaction conditions, the growth rate of O_3-based ALD is often lower than for H_2O and decreases with higher deposition temperature. The difference in ALD efficiency between O_3 and H_2O suggests dramatically different reaction mechanisms and surface chemistry.

Despite the interest in and importance of O_3 as an ALD oxygen source, the surface reaction mechanism is not well understood. On the basis of cluster model DFT calculations and mass spectroscopy measurements, an initial report by Schröder and co-workers[7] suggested that O_3 reacted with surface dimethylaluminum (-$Al(CH_3)_2$) leading to release of ethene (C_2H_4), which ultimately produced surface hydroxyl groups in preparation for reaction with TMA. Subsequent work by Elliott et al.,[8] combining experimental O_3/TMA ALD and DFT simulations also adopted a O_3 surface reaction pathway leading to the desorption of C_2H_4, proceeding from an initial reaction step involving the oxidation of surface methyl groups. They concluded that the relative O_3 ALD growth rate behavior could be attributed to an inhomogeneous -OH surface distribution and the thermal desorption of H_2O at higher temperatures. Recently, Goldstein and George presented a preliminary study using IR spectroscopy to investigate surface reactions during O_3/TMA growth of Al_2O_3 on nanopowders.[9]

Here, we study the initial Al_2O_3 growth mechanism using ozone and identify the formation of an intermediate that bears on the relative efficiency of O_3 as an ALD precursor. Using in situ transmission Fourier transform infrared spectroscopy (FTIR), formate is detected after ozone exposure (second part of the TMA/O_3 ALD cycle), resulting from the further oxidation of surface methoxy groups. To support the observed IR band assignments, vibrational calculations using the density functional theory (DFT) code DMol3 are carried out,[10] using all-electron calculations with the gradient-corrected PBE[11] functional along with a double numeric polarized basis set (DNP). The vibrational modes associated with O_3 ALD surface structures are calculated using fully periodic Al_2O_3 surface models, as well as simple cluster models, for comparison with experimental data.[12]

The initial reaction mechanisms are inferred from vibrational spectra as follows. First, the intensity of the sharp Si−H stretching mode at 2083 cm^{-1} (not shown in Figure

* Corresponding author. E-mail: jinhee@utdallas.edu.
† University of Texas at Dallas.
‡ Rutgers University.
§ Accelrys Inc.

(1) (a) Manasevit, H. M. *J. Electrochem. Soc.* **1971**, *118*, 647. (b) Demchuk, A.; Simpson, S.; Koplitz, B. *J. Phys. Chem. A* **2003**, *107*, 1727.
(2) (a) Schmidt, J.; Risse, T.; Hamann, H.; Freund, H. J. *J. Chem. Phys.* **2002**, *116*, 10861. (b) Anwander, R.; Palm, C.; Groeger, O.; Engelhardt, G. *Organometallics* **1998**, *17*, 2027.
(3) (a) Wilk, G. D.; Wallace, R. M.; Anthony, J. M. *J. Appl. Phys.* **2001**, *89*, 5243. (b) Biercuk, M. J.; Monsma, D. J.; Marcus, C. M.; Becker, J. S.; Gordon, R. G. *Appl. Phys. Lett.* **2003**, *83*, 2405. (c) Ye, P. D.; Wilk, G. D.; Yang, B.; Kwo, J.; Gossmann, H.-J.; Hong, M.; Ng, K. K.; Bude, J. *Appl. Phys. Lett.* **2004**, *84*, 434.
(4) (a) George, S. M.; Ott, A. W.; Klaus, J. W. *J. Phys. Chem.* **1996**, *100*, 13121. (b) Matsuwaki, T.; Nakajimia, T.; Yamashita, K. *J. Phys. IV* **2001**, *11*, 63. (c) Gosset, J. G.; Damlencourt, J.-F.; Renault, O.; Rouchon, D.; Holloger, Ph.; Ermolieff, A.; Trimaille, I.; Ganem, J.-J.; Frank, F.; Semeria, M.-N. *J. Non-Cryst. Solids* **2002**, *303*, 17. (d) Halls, M. D.; Raghavachari, K. *J. Phys. Chem. B* **2004**, *108*, 4058. (e) Puurunen, R. L. *J. Appl. Phys.* **2005**, *97*, 121301. (f) Dallera, C.; Fracassi, F.; Braicovich, L.; Scarel, G.; Wiemer, C.; Fanciulli, M.; Pavia, G.; Cowie, B. C. C. *Appl. Phys. Lett.* **2006**, *89*, 183521.
(5) (a) Wang, Y.; Dai, M.; Ho, M.-T.; Wielunski, L. S.; Chabal, Y. J. *Appl. Phys. Lett.* **2007**, *90*, 022906. (b) Kim, J. B.; Kwon, D. R.; Chakrabarti, K.; Lee, C.; Oh, K. Y.; Lee, J. H. *J. Appl. Phys.* **2002**, *92*, 6739.
(6) (a) Cho, M.; Park, H. B.; Park, J.; Lee, S. W.; Hwang, C. S.; Jeong, J.; Kang, H. S.; Kim, Y. W. *J. Electrochem. Soc.* **2005**, *152*, F49. (b) Kim, S. K.; Lee, S. W.; Hwang, C. S.; Min, Y. S.; Won, J. Y.; Jeong, J. *J. Electrochem. Soc.* **2006**, *153*, F69.
(7) Prechtl, G.; Kersch, A.; Icking-Konert, G. S.; Jacobs, W.; Hecht, T.; Boubekeur, H.; Schröder, U. *IEEE Int. Electron Devices* **2003**, *9*, 6–1.
(8) Elliott, S. D.; Scarel, G.; Wiemer, C.; Fanciulli, M.; Pavia, G. *Chem. Mater.* **2006**, *18*, 3764.
(9) Goldstein, G. N.; George, S. M. *Conference Program of the 6th International Conference on Atomic Layer Deposition*, Seoul, South Korea; American Vacuum Society: New York, 2006.
(10) Delley, B. *J. Chem. Phys.* **2000**, *113*, 7756.
(11) Perdew, J. P.; Burke, K.; Ernzerhof, M. *Phys. Rev. Lett.* **1996**, *77*, 3865.

10.1021/cm703667h CCC: $40.75
Published on Web 05/02/2008

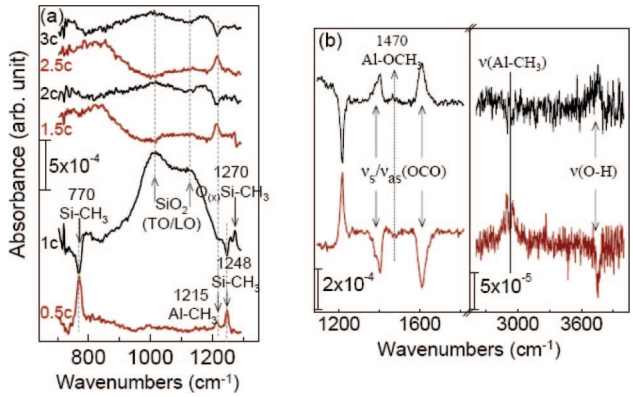

Figure 1. (a) In situ differential FTIR spectra of H/Si(111) exposed to sequential pulses of TMA (0.5c, 1.5c, 2.5c) and ozone (1c, 2c, 3c) at 300 °C up to the third ALD cycle and (b) the differential spectra of the 18.5th referenced to that of the 18th cycle (TMA, red curve) and the 19th referenced to that of the 18.5th cycle (ozone, black curve).

1) is observed to decrease by ~80% after the first TMA pulse, confirming that TMA chemically reacts with the atomically flat H-terminated Si(111) surface as previously reported.[13] Second, the absorption of the methyl deformation mode (observed at 1215 cm^{-1} with a shoulder at 1206 cm^{-1} in Figure 1a) is a useful indicator of the bonding environment. According to a single unit cell cluster calculation, the CH_3 umbrella mode of Si−O−Al-CH_3 is ~6 cm^{-1} higher than that of Si−Al−CH_3. This suggests that Al-CH_3 of TMA is attached to Si atoms either directly or through O atoms. The oxygen insertion, as evidenced also by a broadband around 1000 cm^{-1} (Si−O and Al−O bonds) has been attributed to oxidation of gas phase TMA by residual water inside of the reactor or in the source. The strong modes at 770 cm^{-1} and 1248 cm^{-1} are assigned to the rocking and symmetric deformation modes of methyl groups bonded to Si, respectively, suggesting that methyl groups from TMA can react directly with Si during the initial cycle. Such methyl groups are very stable and most likely cause for C contamination of the interface as discussed below.

The ozone reaction with Si-CH_3 and Si−Al−CH_3 (or Si−O−Al-CH_3) are indeed different as evident after the first full cycle (labeled "1c") in Figure 1a. Ozone attacks the surface Al−C bond, as evidenced by the disappearance of the (O)Al-CH_3 band at 1206−1215 cm^{-1}, but does not eliminate the Si-CH_3 bending mode at 1248 cm^{-1}, which is merely shifted toward ~1270 cm^{-1} because of the oxygen insertion into all three Si backbonds. This indicates that a complete (~1 ML) interfacial oxide layer has been formed, as confirmed by the presence of SiO_2 phonon modes in the 1000−1200 cm^{-1} region. This oxide phonon band is disrupted after each TMA pulse (see intensity loss in spectra "1.5c" and "2.5c") because of the chemical bonding between the surface Si−O−Si matrix and TMA.

For comparison, a H/Si(111) surface was exposed to the same amount of ozone. The integrated area of the resulting SiO_x band was found to be similar to that formed by ozone exposure of a previously TMA-exposed H/Si(111) surface. The presence of a partial methyl layer therefore does not significantly prevent silicon oxidation by ozone.

The presence and evolution of sharp vibrational modes in the 1200−1700 cm^{-1} spectral region upon sequential TMA and ozone exposures provide information for understanding the reaction of O_3. Figure 1b shows the differential IR spectra of the subsequent 19th TMA and ozone exposure. Upon ozone exposure, several new bands are observed to accompany the quenching of the -Al$(CH_3)_2$ bending mode at 1217 cm^{-1}. A weak band at ~1470 cm^{-1} indicates the presence of methoxy species (-Al$(OCH_3)_2$) on the surface after an ozone pulse. Importantly, two strong bands at ~1400 and 1610 cm^{-1} give clear evidence for the presence of formate ($^-$OOCH) at the surface.[9] The band at 1610 cm^{-1} is assigned to the asymmetric OCO stretching vibration, whereas the band at ca. 1400 cm^{-1} is composed of subbands at 1405, 1385 and 1360 cm^{-1}. Those bands are assigned to OCO deformation, CH in-plane bending and the symmetric OCO stretching vibration of the formate species, respectively.[14,15] At 300 °C, the formate species can decompose to gas-phase CO, producing OH groups on the surface (discussed below).[16] These hydroxyl groups out of the formate decomposition are most likely the origin of the OH stretching band at 3750 cm^{-1} after each ozone pulse.

To support these assignments and rule out other known surface species, we have carried out periodic and cluster-based calculations. Figure 2a shows the calculated vibrational density of states from periodic Al_2O_3 surface models and Figure 2b shows the computed vibrational frequencies with corresponding intensities from cluster adsorbate models, along with the experimental spectra (top panel) for comparison. The shaded vertical areas represent characteristic wavenumber regions and are included to facilitate comparison between the experiment and theory. The surface species considered in the calculations include methyl -Al$(CH_3)_2$ (red bar), methoxy -Al$(OCH_3)_2$ (yellow bar), formate -Al(OOCH) (gray bars) and hydroxyl -Al$(OH)_2$. Comparison of the observed IR spectra with the computed spectra for both the periodic (Figure 2a) and cluster models (Figure 2b) supports the assignments made here. The predicted frequencies for the -Al$(CH_3)_2$ umbrella modes at 1211−1240 cm^{-1} can be compared with the observed frequency at 1217 cm^{-1}. The computed frequencies of 1473−1483 cm^{-1} for the methoxy species correspond to the -Al$(OCH_3)_2$ deformation seen in the IR at 1470 cm^{-1}.

As shown in Figure 2, only the formate surface structure is predicted to have vibrational modes at both ~1400 and 1610 cm^{-1}. The symmetric and asymmetric OCO stretching vibrations are calculated to be at 1350 and 1622 cm^{-1}, respectively, in good agreement with experimental values (1360 and 1610 cm^{-1}). In general, there are two different

(12) Periodic atomistic models were based on a 5-layer slab of the (001)-Al_2O_3 surface. Calculations were carried out for the -Al$(CH_3)_2$, -Al$(OCH_3)_2$, -Al$(OH)_2$, and -Al(OOCH) species using 2×1 and 2×2 supercells, respectively, with a 20 Å vacuum slab. A Monkhorst-Pack k-point mesh with a spacing of 0.04 $Å^{-1}$ was used to sample the Brillouin zone. For the cluster models, cluster stoichiometries of $Al_2O_3H_2$-$(CH_3)_2$, $Al_2O_3H_2$-$(OCH_3)_2$, $Al_2O_3H_2$-$(OH)_2$, and Al_2O_3-$(OOCH)_2$ were used.

(13) Frank, M. M.; Chabal, Y. J.; Wilk, G. D. *Appl. Phys. Lett.* **2003**, *82*, 4758.

(14) Boiadjiev, V.; Tysoe, W. T. *Chem. Mater.* **1998**, *10*, 334.

(15) Lopez, S. Y. R.; Rodriguez, J. S.; Sueyoshi, S. S. *Adv. Technol. Mater. Mater. Process. J.* **2006**, *8*, 55.

(16) Hussein, G. A. M.; Sheppard, N. *J. Chem. Soc., Faraday Tran.* **1991**, *87*, 2655.

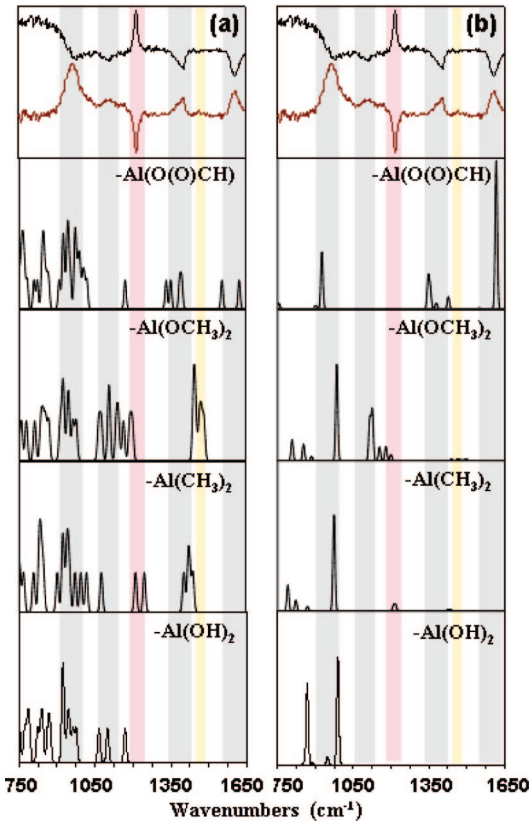

Figure 2. Periodic model vibrational density of states (VDOS) (a) and cluster model IR calculations (b) of each surface structure. The top differential spectra are the same experimental data as in Figure 1b.

formate−aluminum bidentate geometries: a chelating structure, in which each formate binds to a single Al center, and a bridging structure, where a formate bridges between two Al centers. The computed ν_{as}(OCO) and ν_s(OCO) modes were comparable for these two possibilities. However, the CH in-plane bending vibration for the chelating structure was ca. 100 cm^{-1} lower than for the bridging structure. The δ(CH) vibration is observed at 1385 cm^{-1} which corresponds to the calculated bridging formate mode at 1393 cm^{-1}.

Our analysis conclusively shows that a major intermediate in the O_3 ALD reaction pathway at TMA derived Al_2O_3 interfaces is the bidentate bridging formate species. Upon O_3 exposure, possible initial surface reaction products include Al-OCH_3 and Al-CH_2OH species. Our calculations show that methoxy is the thermodynamically preferred product by 1.54 eV, in agreement with previous work by Elliott et al.[8] Formate is a known intermediate in the catalytic decomposition of methanol over metal-oxide catalysts.[17] Interestingly, methanol adsorption on metal-oxides leads to the formation

Table 1. Observed and Calculated Vibrational Frequencies (cm^{-1}) and Band Assignments for the O_3/TMA ALD Surface Formate; Experimental Data for Formate from Other Al_2O_3 Surfaces Included for Comparison

		Al_2O_3/MeOH			
obsd	calcd[a]	ref 14	ref 17a	ref 17b	mode
1360	1350	1368	1378	1377	ν_s (OCO)
1385	1393	1395	1393	1394	δ (CH)
1610	1622	1600	1596	1597	ν_{as} (OCO)

[a] PBE/DNP calculated frequencies of a 2×2 Al_2O_3 supercell with OOCH adsorbate in bridging mode.

of surface methoxy species, similar to those produced during the initial Al_2O_3 ALD process. The formation of formate during Al_2O_3 ALD may be enhanced as O_3 has been shown to dissociatively adsorb on acidic oxides such as Al_2O_3 evolving O_2 and depositing reactive atomic oxygen,[18] which can readily react with coadsorbed methoxy forming formate at 300 °C. As summarized in Table 1, the characteristic O_3 ALD formate wavenumbers reported here compare well with those measured in previous studies of the catalytic decomposition of methanol over Al_2O_3 substrates.[14,17]

Unaided, formate can decompose along two pathways, resulting in release of either CO or CO_2. Acidic oxides such as Al_2O_3 are believed to selectively promote the dehydration of formate to CO and H_2O; particularly in cases where there is an oxygen deficiency in the surface layer.[19] The previously proposed O_3 ALD reaction mechanism[7] was largely motivated by the detection of a signal of mass 28 u upon O_3 exposure, interpreted to be due to loss of C_2H_4. However, CO also has a mass of 28 u. A recent mass spectroscopy study by Kessels and co-workers[20] examined the related TMA/O_2-plasma ALD process. They determined that in the O_2-plasma half-reaction, CO, CO_2, and H_2O were the main reaction products.

The results presented here corroborate and extend initial efforts[9] to critically examine the key species in the O_3/TMA ALD process. The reaction mechanism for O_3 ALD is much more complex than might be assumed. Ligand oxidation to formate and subsequent decompositon to volatile CO_n species results in active O depletion of the growing Al_2O_3 film, severely limiting the final surface hydroxyl density.

Acknowledgment. This research was supported by the National Science Foundation (CHE-0415652). The authors are grateful to S. M. George for his presentations at ALD conferences and many stimulating discussions.

CM703667H

(17) (a) McInroy, A. R.; Lundie, D. T.; Winfield, J. M.; Dudman, C. C.; Jones, P.; Lennon, D. *Langmuir* **2005**, *21*, 11092. (b) Greenler, R. *J. Chem. Phys.* **1962**, *37*, 2094. (c) Busca, G. *Catal. Today* **1996**, *27*, 457. (d) Clarke, D. B.; Lee, D.; Sandoval, M. J.; Bell, A. T. *J. Catal.* **1994**, *150*, 81. (e) Fisher, I. A.; Bell, A. T. *J. Catal.* **1999**, *184*, 357. (f) Sakakini, B.; Tabatabaei, J.; Watson, M.; Waugh, K.; Zemicael, F. W. *Faraday Discuss.* **1996**, *105*, 369.

(18) (a) Bulanin, K. M.; Lavalley, J. C.; Tsyganenko, A. A. *J. Phys. Chem.* **1995**, *99*, 10294. (b) Bulanin, K. M.; Lavalley, J.C.And.; Tsyganenko, A. A. *Colloids Surf., A* **1995**, *101*, 153.

(19) (a) Mars, P.; Scholten, J. J. F.; Zwietering, P. *Adv. Catal.* **1963**, *14*, 35. (b) Morikawa, Y.; Takahashi, I.; Aizawa, M.; Namai, Y.; Sasaki, T.; Iwasawa, Y. *J. Phys. Chem. B* **2004**, *108*, 14446. (c) Patermarakis, G. *Appl. Catal., A* **2003**, *252*, 231.

(20) Heil, S. B. A.; Kudlacek, P.; Langereis, R.; Engeln, R.; van de Sanden, M.C.M.and.; Kessels, W. M. M. *Appl. Phys. Lett.* **2006**, *89*, 131505.